

## MONTE CARLO METHOD FOR MODELING OF ELECTRON TRANSPORT IN QUANTUM WIRES

T. Gurov and E. Atanassov, IPP, Bulgarian Academy of Sciences, Sofia, Bulgaria  
M. Nedjalkov and V. Palankovski, AMADEA Group, IuE, TU Vienna, Austria

Corresponding author: T. Gurov  
IPP, Bulgarian Academy of Sciences  
Acad. G. Bontchev Str., Bl. 25A, 1113 Sofia, Bulgaria  
Phone: +359 2 979-6639, Fax: +359 2 870-7273  
email: gurov@parallel.bas.bg

**Abstract.** We consider a physical model of ultrafast evolution of an initial electron distribution in a quantum wire. The electron evolution is described by a quantum-kinetic equation accounting for the interaction with phonons. A Monte Carlo method has been developed for solving the equation. GRID technologies are implemented due to the large computational efforts imposed by the quantum character of the model.

### 1. Introduction

The Monte Carlo (MC) methods provide approximate solutions to a variety of mathematical problems by performing statistical sampling experiments on a computer. They are based on the simulation of random variables whose mathematical expectations are equal to a given functional of the solution of the problem under consideration.

Many problems in a transport theory and related areas can be described mathematically by a second kind integral equation:

$$f = \mathbb{K}(f) + \phi. \quad (1)$$

In general, the physical quantities of interest are determined by functionals of the type:

$$J_g(f) \equiv (g, f) = \int_G g(x)f(x)dx, \quad (2)$$

where the domain  $G \subset \mathbb{R}^d$  and a point  $x \in G$  is a point in the Euclidean space  $\mathbb{R}^d$ . The functions  $f(x)$  and  $g(x)$  belong to any Banach space  $X$  and to the adjoint space  $X^*$ , respectively, and  $f(x)$  is the solution of (1).

The mathematical concept of the MC approach is based on the iterative expansion of the solution of (1):

$$f_s = \mathbb{K}(f_{s-1}) + \phi, \quad s = 1, 2, \dots, \quad (3)$$

where  $s$  is the number of iterations. In fact (3) defines a Neumann series

$$f_s = \phi + \mathbb{K}(\phi) + \dots + \mathbb{K}^{s-1}(\phi) + \mathbb{K}^s(f_0), \quad s > 1,$$

where  $\mathbb{K}^s$  means the  $s$ -th iteration of  $\mathbb{K}$ . In the case when the corresponding infinite series converges then the sum is an element  $f$  from the space  $X$  which satisfies (1).

The Neumann series, replaced in (2), gives rise to a sum of consecutive terms which are evaluated by the MC method with the help of random estimators. A random variable  $\xi$  is defined as a MC estimator for the functional (2) if the mathematical expectation of  $\xi$  is equal to  $J(f)$ :  $E\xi = J(f)$ .

Therefore we can define a MC method

$$\bar{\xi} = \frac{1}{N} \sum_{i=1}^N \xi^{(i)} \xrightarrow{P} J_g(f), \quad (4)$$

where  $\xi^{(1)}, \dots, \xi^{(N)}$  are independent values of  $\xi$  and  $\xrightarrow{P}$  means stochastic convergence as  $N \rightarrow \infty$ . The rate of convergence is evaluated by the "law of the three sigmas", [1, 2]:

$$P \left( |\bar{\xi} - J_g(f)| < 3 \frac{\sqrt{\text{Var}(\xi)}}{\sqrt{N}} \right) \approx 0.997.$$

Here  $Var(\xi) = E\xi^2 - E^2\xi$  is the variance of the MC estimator. Thus, a peculiarity of any MC estimator is that the result is obtained with a statistical error [1, 2, 3]. As  $N$  increases, the statistical error decreases proportionally to  $N^{-1/2}$ .

Thus, there are two types of errors - systematic (a truncation error) and stochastic (a probability error) [3, 4]. The systematic error depends on the number of iterations of the used iterative method, while the stochastic error is related to the probabilistic nature of the MC method. From (1) and (3) one can get the value of the truncation error. If  $f_0 = \phi$  then

$$f_s - f = \mathbb{K}^s(\phi - f).$$

The relation (4) still does not determine the computational MC algorithm: we must specify the modeling function (called sampling rule)

$$\Theta = F(\beta_1, \beta_2, \dots), \quad (5)$$

where  $\beta_1, \beta_2, \dots$ , are uniformly distributed random numbers in the interval  $(0, 1)$ . It is known that random number generators are used to produce such sequences of numbers. They are based upon specific mathematical algorithms, which are repeatable and sequential. Now both relations (4) and (5) define a MC algorithm for estimating  $J_g(f)$ . The case when  $g = \delta(x - x_0)$  is of special interest, because it is considered for calculating the value of  $f$  at  $x_0$ , where  $x_0 \in G$  is a fixed point.

Every iterative algorithm uses a finite number of iterations  $s$ . In practice we define a MC estimator  $\xi_s$  for computing the functional  $J_g(f_s)$  with a statistical error. On the other hand  $\xi_s$  is a biased estimator for the functional  $J_g(f)$  with stochastic and truncation errors. The number of iterations can be a random variable when an  $\varepsilon$ -criterion is used to truncate the Neumann series or the corresponding Markov chain in the MC algorithm.

The stochastic convergence rate is approximately  $O(N^{-1/2})$ . In order to accelerate the convergence rate of the MC methods several techniques have been developed. Variance reductions techniques, like antithetic varieties, stratification and importance sampling [2], reduce the variance which is a quantity to measure the probabilistic uncertainty. Parallelism is another way to accelerate the convergence of the MC computations. If  $n$  processors execute  $n$  independent MC computations using non-overlapping random sequences, the accumulated result has a variance  $n$  time smaller than that of a single copy. In our work we use SPRNG (Scalable Parallel Random Number Generators) library [5] to produce independent random streams. The numerical results presented in Section 4 are obtained at the Bulgarian Grid-computing systems that are part of EGEE-GRID [6].

The paper is organized as follows. In Section 2 the quantum-kinetic equation is derived from a physical model describing electron transport in quantum wires. An integral form of the equation is obtained by reducing the dimensionality of space and momentum coordinates. The MC method and corresponding MC algorithm are presented in Section 3. The numerical results using Grid implementation are discussed in Section 4. Summary and directions for future work are given in Section 5.

## 2. The Physical Model

We consider a highly non-equilibrium electron distribution which propagates in a quantum semiconductor wire. The electrons, which can be initially injected or optically generated in the wire, begin to interact with three-dimensional phonons. The direction of the wire is chosen to be  $z$ , the corresponding component of the wave vector is  $k_z$ . The electrons are in the ground state  $\Psi(\mathbf{r}_\perp)$  in the plane normal to the wire, which is an assumption consistent at low temperatures. In general, an electric field  $\mathbf{F}$  can be applied along  $z$ . Here we consider the case  $\mathbf{F} = 0$ .

The equation the relevant for the evolution process is derives by a first principle approach in terms of the electron Wigner function  $f_w$ .

$$\begin{aligned} f_w(z, k_z, t) = & f_{w0}(z - \frac{\hbar k_z}{m}t, k_z) + \\ & + \int_0^t dt'' \int_{t''}^t dt' \int_G d^3\mathbf{k}' \{K_1(k_z, \mathbf{k}', t', t'') f_w(z + \hbar(k_z, q'_z, t, t'), k'_z, t'')\} \\ & + \int_0^t dt'' \int_{t''}^t dt' \int_G d^3\mathbf{k}' \{K_2(k_z, \mathbf{k}', t', t'') f_w(z + \hbar(k_z, q'_z, t, t'), k_z, t'')\}, \end{aligned} \quad (6)$$

where

$$\begin{aligned} h(k_z, q'_z, t, t'') &= -\frac{\hbar k_z}{m}(t - t'') + \frac{\hbar q'_z}{2m}(t' - t''), \\ K_1(k_z, \mathbf{k}', t', t'') &= S(k'_z, k_z, t', t'', \mathbf{q}'_\perp) = -K_2(\mathbf{k}', k_z, t', t''), \end{aligned}$$

$$S(k'_z, k_z, t', t'', \mathbf{q}'_\perp) = \frac{2V}{(2\pi)^3} |G(\mathbf{q}'_\perp) \mathcal{F}(\mathbf{q}'_\perp, k_z - k'_z)|^2 \times \\ \left[ (n(\mathbf{q}') + 1) \cos\left(\frac{\epsilon(k_z) - \epsilon(k'_z) + \hbar\omega_{\mathbf{q}'}}{\hbar}(t' - t'')\right) \right. \\ \left. + n(\mathbf{q}') \cos\left(\frac{\epsilon(k_z) - \epsilon(k'_z) - \hbar\omega_{\mathbf{q}'}}{\hbar}(t' - t'')\right) \right]$$

where  $\int_G d^3\mathbf{k}' = \int d\mathbf{q}'_\perp \int_{-Q_2}^{Q_2} dk_z$  and the domain  $G$  is specified in the next section. The phonon distribution is described by the Bose function,  $n_{\mathbf{q}'} = 1/(\exp(\hbar\omega_{\mathbf{q}'}/KT) - 1)$  with  $K$  the Boltzmann constant and  $T$  is the temperature of the crystal.  $\hbar\omega_{\mathbf{q}'}$  is the phonon energy which generally depends on  $\mathbf{q}' = \mathbf{q}'_\perp + q'_z = \mathbf{q}'_\perp + (k_z - k'_z)$ , and  $\epsilon(k_z) = (\hbar^2 k_z^2)/2m$  is the electron energy. The electron-phonon coupling constant  $\mathcal{F}$  is chosen according to a Fröhlich polar optical interaction:

$$\mathcal{F}(\mathbf{q}'_\perp, k_z - k'_z) = - \left[ \frac{2\pi e^2 \omega_{\mathbf{q}'}}{\hbar V} \left( \frac{1}{\epsilon_\infty} - \frac{1}{\epsilon_s} \right) \frac{1}{(\mathbf{q}')^2} \right]^{\frac{1}{2}}, \quad (7)$$

( $\epsilon_\infty$ ) and ( $\epsilon_s$ ) are the optical and static dielectric constants.  $G(\mathbf{q}'_\perp)$  is the Fourier transform of the square of the ground state wave function  $|\Psi|^2$ .

The equation describes electron evolution which is quantum in both, the real space due to the confinements of the wire, and the momentum space due to the early stage of the electron-phonon kinetics. The kinetics resembles the memory character of the homogeneous Levinson or Barker-Ferry models [7, 8], but the evolution problem becomes inhomogeneous due to the spatial dependence of the initial condition  $f_{w0}$ . The cross-section of the wire is chosen to be a square with side  $a$  so that:

$$|G(\mathbf{q}'_\perp)|^2 = |G(q'_x)G(q'_y)|^2 = \left( \frac{4\pi^2}{q'_x a ((q'_x a)^2 - 4\pi^2)} \right)^2 4 \sin^2(aq'_x/2) \left( \frac{4\pi^2}{q'_y a ((q'_y a)^2 - 4\pi^2)} \right)^2 4 \sin^2(aq'_y/2)$$

We note that the Neumann series of integral equations of type (6) converges, [9]. Thus, we can construct a MC estimator to evaluate suitable functionals of the solution.

### 3. The Monte Carlo Method

The values of the physical quantities are expressed by the following general functional of the solution of (6):

$$J_g(f) \equiv (g, f) = \int_0^T \int_D g(z, k_z, t) f_w(z, k_z, t) dz dk_z dt. \quad (8)$$

Here we specify that the phase space point  $(z, k_z)$  belongs to a rectangular domain  $D = (-Q_1, Q_1) \times (-Q_2, Q_2)$ , and  $t \in (0, T)$ . The function  $g(z, k_z, t)$  depends on the quantity of interest. In particular, we focus on the Wigner function (6), the wave vector (and respectively the energy)  $f(k_z, t)$ , and the density distribution  $n(z, t)$ . The latter two functions are given by the integrals

$$f(k_z, t) = \int \frac{dz}{2\pi} f_w(z, k_z, t); \quad n(z, t) = \int \frac{dk_z}{2\pi} f_w(z, k_z, t). \quad (9)$$

The evaluation is performed in fixed points by choosing  $g(z, k_z, t)$  as follows:

$$(i) \quad g(z, k_z, t) = \delta(z - z_0) \delta(k_z - k_{z,0}) \delta(t - t_0), \\ (ii) \quad g(z, k_z, t) = \frac{1}{2\pi} \delta(k_z - k_{z,0}) \delta(t - t_0), \\ (iii) \quad g(z, k_z, t) = \frac{1}{2\pi} \delta(z - z_0) \delta(t - t_0). \quad (10)$$

We construct a biased MC estimator for evaluating the functional (8) using backward time evolution of the numerical trajectories in the following way:

$$\xi_s[J_g(f)] = \frac{g(z, k_z, t)}{p_{in}(z, k_z, t)} W_0 f_w(\cdot, k_z, 0) + \frac{g(z, k_z, t)}{p_{in}(z, k_z, t)} \sum_{j=1}^s W_j^\alpha f_w(\cdot, k_{z,j}^\alpha, t_j), \quad (11)$$

where

$$f_w(\cdot, k_{z,j}^\alpha, t_j) = \begin{cases} f_w(z + h(k_{z,j-1}, q'_{z,j}, t_{j-1}, t'_j, t_j), k_{z,j}, t_j), & \text{if } \alpha = 1, \\ f_w(z + h(k_{z,j-1}, q'_{z,j}, t_{j-1}, t'_j, t_j), k_{z,j-1}, t_j), & \text{if } \alpha = 2, \end{cases}$$

$$W_j^\alpha = W_{j-1}^\alpha \frac{K_\alpha(k_{z,j-1}, \mathbf{k}_j, t'_j, t_j)}{p_\alpha p_{tr}(\mathbf{k}_{j-1}, \mathbf{k}_j, t'_j, t_j)}, \quad W_0^\alpha = W_0 = 1, \quad \alpha = 1, 2, \quad j = 1, \dots, s.$$

The probabilities  $p_\alpha$ , ( $\alpha = 1, 2$ ) are chosen to be proportional to the absolute value of the kernels in (6). The initial density  $p_{in}(z, k_z, t)$  and the transition density  $p_{tr}(\mathbf{k}, \mathbf{k}', t', t'')$  are chosen to be tolerant<sup>1</sup> to the given function  $g(z, k_z, t)$  and the kernels, respectively. The first point  $(z, k_{z0}, t_0)$  in the Markov chain is chosen using the initial density, where  $k_{z0}$  is the third coordinate of the wave vector  $\mathbf{k}_0$ . Next points  $(k_{zj}, t'_j, t_j) \in (-Q_2, Q_2) \times (t_j, t_{j-1}) \times (0, t_{j-1})$  of the Markov chain:

$$(k_{z0}, t_0) \rightarrow (k_{z1}, t'_1, t_1) \rightarrow \dots \rightarrow (k_{zj}, t'_j, t_j) \rightarrow \dots \rightarrow (k_{zs}, t'_s, t_s), \quad j = 1, 2, \dots, s$$

do not depend on the position  $z$  of the electrons. They are sampled using the transition density  $p_{tr}(\mathbf{k}, \mathbf{k}', t', t'')$  as we take only the  $k_z$ -coordinate of the wave vector  $\mathbf{k}$ . Note the time  $t'_j$  conditionally depends on the selected time  $t_j$ . The Markov chain terminates in time  $t_s < \varepsilon_1$ , where  $\varepsilon_1$  is a fixed small positive number called a truncation parameter. In order to evaluate the functional (8) by  $N$  independent samples of the estimator (11), we define a Monte Carlo method

$$\frac{1}{N} \sum_{i=1}^N (\xi_s[J_g(f)])_i \xrightarrow{P} J_g(f(s)) \approx J_g(f). \quad (12)$$

$f(s)$  is the iterative solution obtained by the Neumann series of (6), and  $s$  is the number of iterations. In order to obtain a MC computational algorithm, we have to specify the initial and transition densities. Also, we have to describe the sampling rule needed to calculate the states of the Markov chain by using SPRNG library.

We note the MC estimator is constructed using the kernels of the equation (6). That is why we suggest the transition density function to be proportional of the term (7) that contains the singularity, namely:  $p_{tr}(\mathbf{k}, \mathbf{k}', t', t'') = p(\mathbf{k}'/\mathbf{k})p(t, t', t'')$ , where

$$p(t, t', t'') = p(t, t'')p(t'/t'') = \frac{1}{t} \frac{1}{(t - t'')}, \quad p(\mathbf{k}'/\mathbf{k}) = c_1/(\mathbf{k}' - \mathbf{k})^2.$$

$c_1$  is the normalized constant. Thus, if we know  $t$ , the next times  $t''$  and  $t'$  are computed by using the inverse-transformation rule. The function  $p(\mathbf{k}'/\mathbf{k})$  is chosen in spherical coordinates  $(\rho, \theta, \varphi)$ , in the following way:  $p(\mathbf{k}'/\mathbf{k}) = (4\pi)^{-1}(\rho)^{-2}l(\omega)^{-1}$ , where  $\omega = (\mathbf{k}' - \mathbf{k})/\rho$ ,  $\rho = |\mathbf{k}' - \mathbf{k}|$  and  $l(\omega)$  is distance in the direction of the unit vector  $\omega$  from  $\mathbf{k}$  to the boundary of the domain  $G$ . If  $G$  is a sphere with radius  $Q_2$ , the function  $p(\mathbf{k}'/\mathbf{k})$  satisfies the condition for a transition density. Indeed,

$$\int_G p(\mathbf{k}'/\mathbf{k}) d^3 \mathbf{k}' = \oint (4\pi)^{-1} d\omega \int_0^{l(\omega)} l(\omega)^{-1} dr' = 1.$$

Thus, if we know the wave vector  $\mathbf{k}$  the next state  $\mathbf{k}'$  can be computed by the following sample rule:

**Algorithm :**

1. **Sample** a random unit vector  $\omega = (\sin \theta \cos \varphi, \sin \theta \sin \varphi, \cos \theta)$  as  $\sin \theta = 2\sqrt{(\beta_1 - \beta_1^2)}$ ,  $\cos \theta = 2\beta_1 - 1$ , and  $\varphi = 2\pi\beta_2$  where  $\beta_1$  and  $\beta_2$  are uniformly distributed numbers in  $(0, 1)$ ;
2. **Calculate**  $l(\omega) = -\omega \cdot \mathbf{k} + (Q_2^2 + (\omega \cdot \mathbf{k})^2 - \mathbf{k}^2)^{\frac{1}{2}}$ , where  $\omega \cdot \mathbf{k}$  means a scalar product between two vectors;
3. **Sample**  $\rho = l(\omega)\beta_3$ , where  $\beta_3$  is an uniformly distributed number in  $(0, 1)$ ;
4. **Calculate**  $\mathbf{k}' = \mathbf{k} + \rho\omega$ .

The choice of  $p_{in}(z, k_z, t)$  depends on the choice of the function  $g(z, k_z, t)$  in (10). Thus, by using common Markov chains the desired physical quantities (values of the Wigner function, the energy and the density distributions) can be evaluated simultaneously.

<sup>1</sup> $r(x)$  is tolerant of  $g(x)$  if  $r(x) > 0$  when  $g(x) \neq 0$  and  $r(x) \geq 0$  when  $g(x) = 0$ .

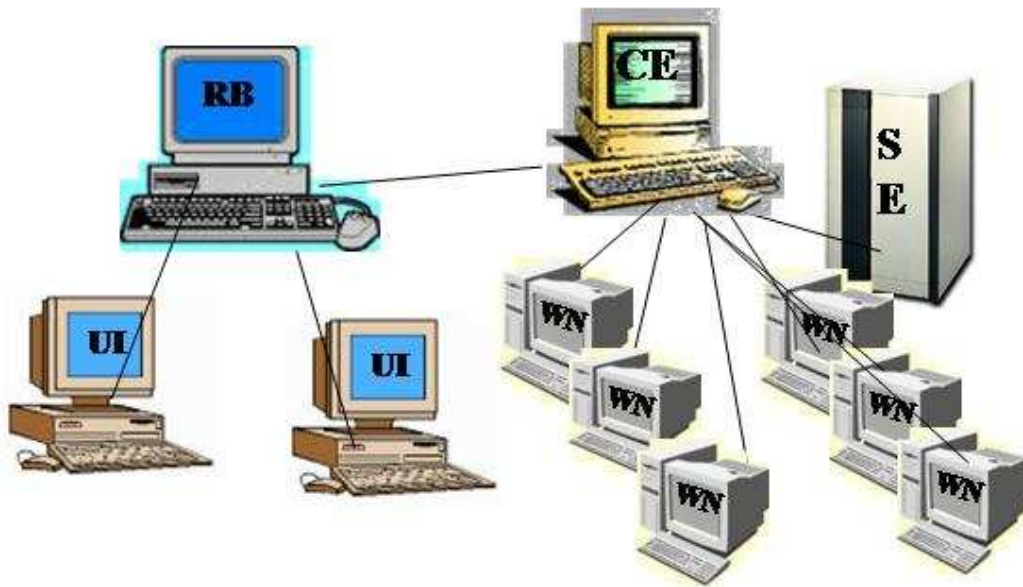


**Figure 1:** The users submit their jobs using *User Interface* (UI) to *Resource Broker* (RB). The *Computing Element* (CE) receives the jobs and controls their execution on the *Worker Nodes* (WNs).

#### 4. Grid implementation and numerical results

The stochastic error for the (homogeneous) Levinson or Barker-Ferry models has order  $O(\exp(c_2 t) N^{-1/2})$ , where  $t$  is the evolution time and  $c_2$  is a constant depending on the kernels of the obtained quantum kinetic equation [9, 10]. Using the same mathematical techniques as in [9], we can prove that the stochastic error of the MC estimator under consideration has order  $O(\exp(c_3 t^2) N^{-1/2})$ . We obtain the term  $t^2$  in the factor  $\exp(c_3 t^2)$  because the quantum kinetic equation (6) contained twice integration on the evolution time. Thus, in our inhomogeneous case the estimate is worse than in the homogeneous one. The estimate shows that when  $t$  is fixed and  $N \rightarrow \infty$  the error decreases, but for large  $t$  the factor  $\exp(c_3 t^2)$  looks ominous. Therefore, the MC algorithm described above solves an  $NP$ -hard problem concerning the evolution time. The suggested importance sampling technique, which overcomes the singularity in the kernels, is not enough to solve the problem for long evolution time with small stochastic error. In order to decrease the stochastic error we have to increase  $N$  - the number of Markov chain realizations. For this aim, a lot of CPU power is needed for achieving acceptable accuracy at evolution times above 100 femtoseconds.

It is known that the MC algorithms are perceived as computationally intensive and naturally parallel [11]. They can usually be implemented via the so-called dynamic *bag-of-work* model [12]. In this model, a large MC task is split into smaller independent subtasks, which are then executed separately. Then, the partial results are collected and used to assemble an accumulated result with smaller variance than that of a single copy. The inherent characteristics of MC algorithms and the dynamic *bag-of-work* model make them a natural fit for the Grid-computing environment.

By using the Grid environment provided by EGEE project middleware <sup>2</sup>, we were able to reduce the computing time of the MC algorithm under consideration. The simulations of the Markov chain are parallelized on the Grid by splitting the underlying random number sequences from the SPRNG library. We divided the MC task into a number of subtasks and submitted them to the EGEE [6] computational grid by the *task-split service* and utilized the grid's *Workload Management Service* (called also *Resource Broker* (RB) in EGEE) to dispatch these independent subtasks to different nodes among EGEE sites (computer clusters) (see Figure 1). The *connectivity services* are

<sup>2</sup>The Enabling Grids for E-science (EGEE) project is funded by the European Commission and aims to build on recent advances in grid technology and develop a service grid infrastructure which is available to scientists 24 hours-a-day. The project aims to provide researchers in both academia and industry with access to major computing resources, independent of their geographic location. The EGEE project identifies a wide-range of scientific disciplines and their applications and supports a number of them for deployment. To date there are five different scientific applications running on the EGEE Grid infrastructure. For more information see <http://public.eu-egee.org/>.

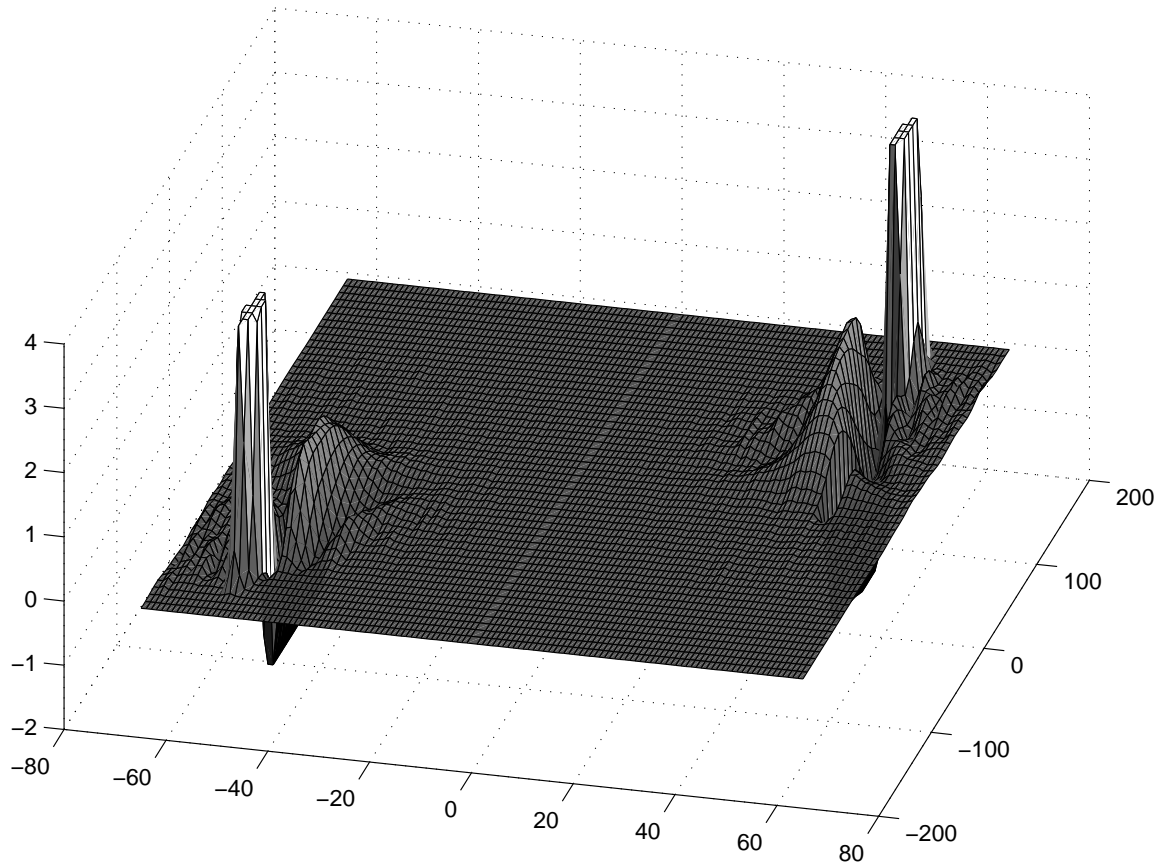


**Figure 2:** The Wigner function solution at  $150fs$  presented in the plane  $z \times k_z$ . A window in the  $z$  domain is chosen for a better resolution.

provided using the *gridftp* protocol. The execution of a subtask takes advantage of the *Storage Elements* to store the executable, intermediate results, and to store each subtask's final (partial) result. When the subtasks are done, the RB and *Logging and Bookkeeping Service* are used to collect the information about the results, and then the *task-gathering service* gets the results of the successfully executed subtasks. The *task-split service* and *task-gathering service* have been prepared by using the SQL language. In our research, the MC algorithm has been implemented in C language. Successful tests of the algorithm were performed at the Bulgarian EGEE Grid sites using the Resource Broker at BG01-IPP Grid site. The BG01-IPP Grid site was also used for the computations, because it has 21 Worker Nodes with 2.8 GHz Pentium IV CPUs. The MPI implementation was MPICH 1.2.6, and the execution is controlled from the Computing Element via the Torque batch system.

The numerical results presented in Figures 2-4 are obtained for zero temperature and GaAs material parameters: the electron effective mass is 0.063, the optimal phonon energy is 36 meV, the static and optical dielectric constants are  $\epsilon_s = 12.9$  and  $\epsilon_\infty = 10.92$ . The initial condition is a product of two Gaussian distributions of the energy and space. The  $k_z^2$  distribution corresponds to a generating laser pulse with an excess energy of about 150 meV. The  $z$  distribution is centered around zero. The side of the wire is chosen to be 10 nanometers.

The solutions of the Wigner function  $f(z, k_z, t)$  are estimated in a rectangular domain  $(-Q_1, Q_1) \times (-Q_2, Q_2)$ , where  $Q_1 = 400 \text{ nm}$  and  $Q_2 = 0.66 \text{ nm}^{-1}$  consisting of  $800 \times 260$  points. The solution for 150 femtoseconds evolution time is shown in Figure 2. Figure 3 demonstrates the process of energy relaxation described by the quantity  $k_z f(k_z, t)$ . The electron density distribution along the wire is shown on Figure 4 for 150 femtoseconds evolution time.

The timing results for evolution time  $t = 100$  femtoseconds are shown in Table 1. The parallel efficiency is close to 100%.

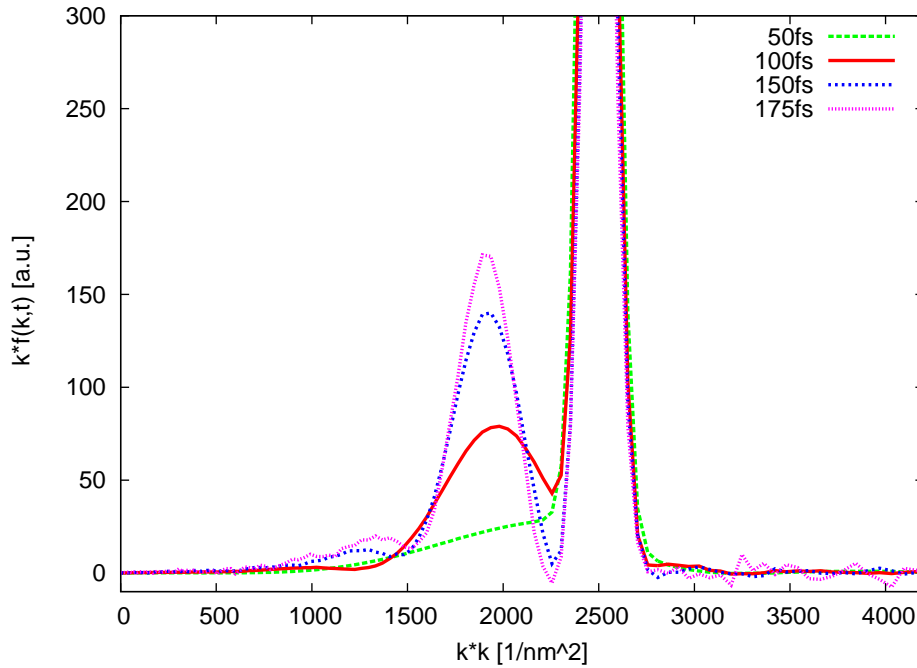


**Figure 3:** Energy relaxation of the highly non-equilibrium initial condition. At  $T = 0$  classical electrons form exact replicas of the initial condition towards low energies. The quantum solution shows broadening of the replicas. Electrons appear in the classically forbidden region above the initial condition. Here the variance of the solution for 175 fs is still high with respect to the solutions for shorter times, obtained with the same computational efforts.

## 5. Conclusion

A quantum-kinetic model for the evolution of an initial electron distribution in a quantum wire has been introduced in terms of the electron Wigner function. The physical quantities, expressed as functionals of the Wigner function are evaluated within a stochastic approach. The developed MC method is characterized by the typical for quantum algorithms computational demands. The stochastic variance grows exponentially with the evolution time and requires implementation of GRID technologies. The EGEE Grid environment has been used to test the MC algorithm on MPI-enabled Grid sites. The test results show excellent parallel efficiency. The next phase of our research will be to obtain results for larger evolution times that require more computational power. This means that the MC algorithm should run on larger sites or on several Grid sites in parallel. Also, the modeling of electron transport in a quantum wire should be investigated in case of an applied electric field.

## Acknowledgment

This work has been supported by the Austrian Science Funds, FWF Project START Y247-N13, by the Bulgarian NSF grant I-1201/02, and by the FP6 INCO Grant 016639/2005, Project BIS 21++.

**Table 1:** The CPU time (seconds) for all  $800 \times 260$  points, the speed-up, and the parallel efficiency. The number of the Markov chain simulations is  $N = 100000$ . The evolution time is 100 fs.

Number of CPUs	CPU Time (s)	Speed-up	Parallel Efficiency
2	9790	-	-
4	4896	1.9996	0.9998
6	3265	2.9985	0.9995

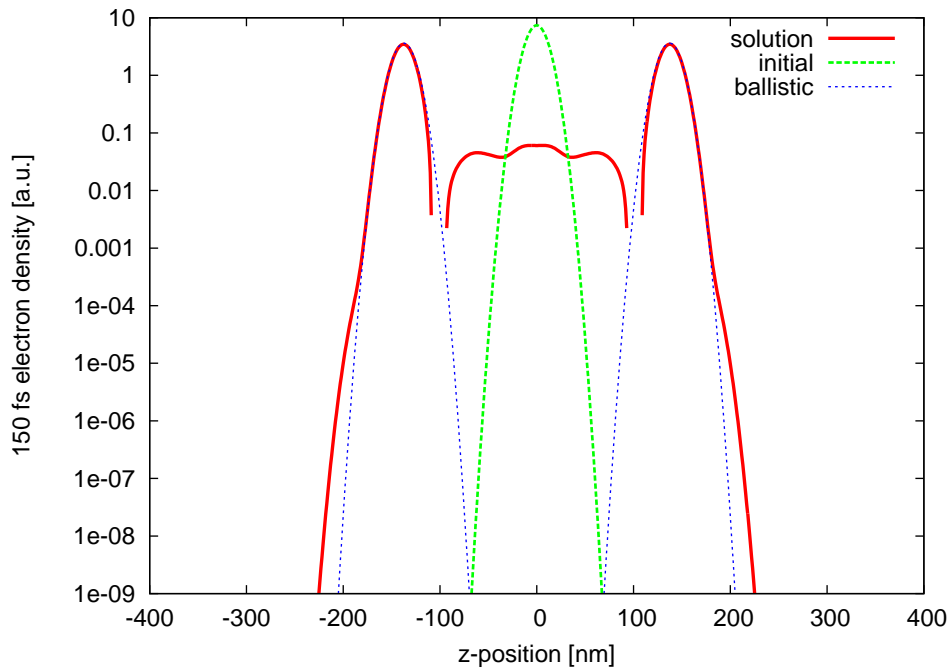


**Figure 4:** Electron density along the wire after 150 fs. The ballistic curve outlines the largest distance which can be reached by classical electrons. The quantum solution reaches larger distances due to the electrons scattered in the classically forbidden energy region.

## References

- [1] I.M. Sobol, Monte Carlo Numerical Methods, (Nauka, Moscow, 1973) (in Russian).
- [2] M.A. Kalos, P.A. Whitlock, Monte Carlo Methods, (Wiley Interscience, New York, 1986).
- [3] G.A. Mikhailov, New Monte Carlo Methods with Estimating Derivatives, (Utrecht, The Netherlands, 1995).
- [4] I. Dimov, T. Dimov, T. Gurov, "A New Iterative Monte Carlo Approach for Inverse Matrix Problem", *J. of Comp. and Appl. Math.*, vol. 92, pp. 15–35, 1998.
- [5] Scalable Parallel Random Number Generators Library for Parallel Monte Carlo Computations, *SPRNG 1.0 and SPRNG 2.0* – <http://sprng.cs.fsu.edu>.
- [6] Enabling Grid for E-scienceE (EGEE), <http://public.eu-egee.org>.
- [7] C. Ringhofer, M. Nedjalkov, H. Kosina, and S. Selberherr, "Semi-Classical Approximation of Electron-Phonon Scattering Beyond Fermi's Golden Rule", *SIAM J. of Appl. Mathematics*, vol. 64, no. 6, pp. 1933–1953, 2004, and the references therein.
- [8] M. Nedjalkov, H. Kosina, S. Selberherr, C. Ringhofer, D.K. Ferry, "Unified Particle Approach to Wigner-Boltzmann Transport in Small Semiconductor Devices", *Phys. Rev. B*, vol. 70, pp. 115319–115335, 2004.
- [9] T.V. Gurov, P.A. Whitlock, "An Efficient Backward Monte Carlo Estimator for Solving of a Quantum Kinetic Equation with Memory Kernel", *Mathematics and Computers in Simulation*, vol. 60, pp. 85–105, 2002.
- [10] T.V. Gurov, M. Nedjalkov, P.A. Whitlock, H. Kosina and S. Selberherr, "Femtosecond Relaxation of Hot" Electrons by Phonon Emission in Presence of Electric Field", *Physica B*, vol. 314, pp. 301–304, 2002.
- [11] I. Dimov, O. Tonev, "Monte Carlo Algorithms: Performance Analysis for Some Computer Architectures", *J. of Comp. and Appl. Mathematics*, vol. 48, pp. 253–277, 1993.
- [12] Y. Li, M. Mascagni, Grid-based Quasi-Monte Carlo Applications, *Monte Carlo Methods and Appl.*, vol. 11, no. 1, pp. 39–56, 2005.